Structural Engineering and Mechanics, *Vol. 68, No. 2 (2018) 227-235*
DOI: https://doi.org/10.12989/sem.2018.68.2.227

A new cable force identification method considering cable flexural rigidity

Long Wang[1,2a], Bo Wu[1a], Junyue Gao[2b], Kairong Shi*[1], Wenzhi Pan[1c], Zhuoyi He[1c], Zhijian Ruan[1c] and Quanpan Lin[1c]

[1]*School of Civil Engineering and Transportation, South China University of Technology, Guangzhou, 510641, P. R. China*
[2]*Guangzhou Construction Co., Ltd, Guangzhou, 510030, P. R. China*

(Received May 6, 2018, Revised August 21, 2018, Accepted August 26, 2018)

Abstract. Cables are the main load-bearing members of prestressed structure and other tensegrity structures. Based on the static equilibrium principle, a new cable force identification method considering cable flexural rigidity is proposed. Its computational formula is derived and the strategy to solve its implicit formula is introduced as well. In order to improve the reliability and practicality of this method, the influence of the cable flexural rigidity on cable force identification accuracy is also investigated. Through cable force identification experiments, the relationships among certain parameters including jacking force, jacking displacement, initial cable force, and sectional area (flexural rigidity) are studied. The results show that the cable force calculated by the proposed method considering flexural rigidity is in good agreement with the finite element results and experimental results. The proposed method with high computational accuracy and resolution efficiency can avoid the influences of the boundary condition and the length of the cable on calculation accuracy and is proven to be conveniently applied to cable force identification in practice.

Keywords: prestressed structure; flexural rigidity; cable force identification method; static equilibrium; experimental research

1. Introduction

Cables are the main load-bearing members of prestressed structure and other tensegrity structures, and the cable force has significantly influence on structural safety (Kim and Kang 2016). It is necessary to detecting the cable force during the process of health monitoring and safety assessment of structures. In order to obtain the actual state of the cable force, choosing a suitable testing method and devices to reduce the interference factor in measurement is the key problem to be solved.

So far, some methods for identify cable force have been proposed, such as tension sensor method (Russel and Lardner 1998), fiber-grating sensor method (Shu *et al.* 2013), frequency method (Wang *et al.* 2015, Rebelo *et al.* 2010, Amabili *et al.* 2010, Xia *et al.* 2017, Sim *et al*. 2014), and magneto-elastic method (Tang *et al.* 2014). In tension sensor and the fiber-grating sensor methods, sensors must be installed before cable tension, and the measuring result is just the force increment after the sensors have been installed. Although the force of in-service cable can be measured with magneto-elastic method, sensors must be placed before tension as well. To measure the force of in-service cable after construction, frequency method is widely used in many countries. However, for the short cable with high frequency or the cable with complex boundary, the application of frequency method is restricted.

Concerning abovementioned problems, the static force testing method is used to identify the cable force. According to mechanical characteristics of prestressed statically determinate structures, Zhang *et al.* (2006) proposed the cable force identification method for string structure but the actual service load is needed, which leads to limitations in practice. In addition, the accuracy of the calculated cable force depends on the estimation accuracy of the actual service load. Furthermore, Tian *et al.* (2013) developed cable force identification method for spoke structural roof based on displacement measurement. In this method, a finite element model is established in accordance with the measuring configuration of the structure, and then the same loads are applied to the actual structure and the finite element model. Finally, the cable force was estimated according to the difference between measured and calculated displacements values. However, the comparative model of this method is difficult to establish. The process of cable force identification is also complicated and the accuracy is hard to guarantee.

Summarizing the existing cable force identification methods, Wang *et al.* (2013) proposed an applicable cable force identification method based on static testing method, cable stress stiffening effect and the principle of static equilibrium. Cable force identification formulas for certain acting locations of jacking force are presented. The calculated cable force in this method is only related to the displacement of jacking force location and the value of jacking force. Compared with the common cable force identification methods, the influences of the boundary

*Corresponding author, Associate Professor
E-mail: krshi@scut.edu.cn
[a]Professor
[b]Senior Engineer
[c]M.Sc. Student

Copyright © 2018 Techno-Press, Ltd.

ISSN: 1225-4568 (Print), 1598-6217 (Online)

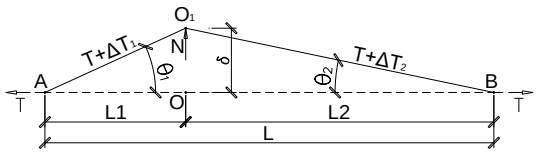

Fig. 1 Cable force identification principle

condition and the length of the cable on calculation accuracy can be avoided in this method. However, the assumption that the cable is supposed to be ideally flexible is difficult to be satisfied in practice.

In this paper, the principle of static equilibrium method is reviewed. A novel cable force identification method based on static equilibrium method is proposed with cable flexural rigidity considering. And its formula and solving method is also introduced. To verify its accuracy, the comparison with the finite element simulation result is conducted. Finally, to assess the influences of the parameters and the accuracy of the proposed method, an experiment for cable force identification is carried out.

2. Basic principle of static equilibrium method

The basic principle of static equilibrium method for cable force identification (Wang *et al.* 2013) is reviewed as follows. The segment of the testing cable is fixed with the cable clamps to avoid relative sliding between the cable and cable clamp. Then with the cable force increasing, the increment of the cable force will not be transferred to the lateral cable segments.

As shown in Fig. 1, L is the distance between the two ends (A and B), and T is the cable force. Jacking force N is applied in the point O. L_1 is the distance between the point O and the left end. Then a jacking displacement δ of the cable segment is induced. In equilibrium state, point O is forced to the point O_1. L_{01} is the original length of the cable segment AO_1. L_{02} is the original length of the cable segment BO_1. ΔT_1 is the cable force increment of the left-side cable segment. ΔT_2 is the cable force increment of the right-side cable segment. θ_1 is the angle of the left-side cable segment, and θ_2 is the angle of the right side cable segment. When the jacking force and the lateral jacking displacement are recorded, Eq. (1) is used to obtain the cable force T.

$$\begin{aligned}\mathrm{T} = &\frac{\cos\theta_1\cos\theta_2\,(L_1+L_2)[N\cos\theta_1+EA\sin(\theta_1+\theta_2)]}{\sin(\theta_1+\theta_2)\{L_1\cos\theta_2\,[N\cos\theta_1+EA\sin(\theta_1+\theta_2)]}\\ &\frac{[N\cos\theta_2+EA\sin(\theta_1+\theta_2)]}{+L_2\cos\theta_1\,[N\cos\theta_2+EA\sin(\theta_1+\theta_2)]\}}-EA\end{aligned} \quad (1)$$

Specifically, when the jacking force is applied in the mid-span of the fixed cable segment, that is, $L_1 = L_2$, and the jacking displacement δ is relatively small compared with the length of the fixed cable segment, Eq. (1) can be simplified as

$$\mathrm{T} = \frac{NL}{4\delta} - 2\left(\frac{\delta}{L}\right)^2 EA \quad (2)$$

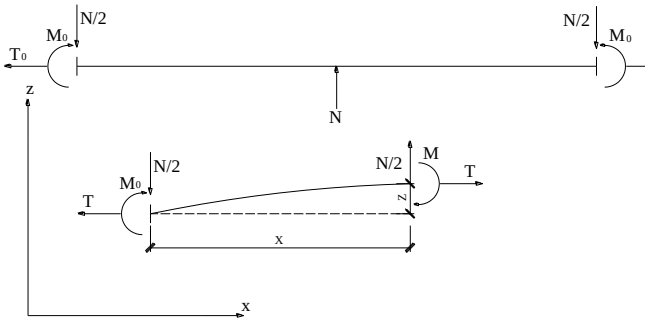

Fig. 2 Mechanical analysis model of the fixed cable segment

where E represents cable elastic modulus. A is cross sectional area of the cable segment. N, δ can be measured by pressure sensor and displacement sensor.

Eq. (2) of cable force identification is obtained by assuming that the cable is in an ideal flexible state. It can be used to test the cable with long fixed cable segment and small cross section. However, for convenient operation or limited field condition in practice, the length of the fixed cable segment is extremely small. Then the fixed cable segment under lateral jacking force behaves obvious characteristics of beam element. Thus, the effect of flexural rigidity cannot be ignored.

3. Computational formula of the cable force identification considering flexural rigidity

Eqs. (1) and (2) present the cable force identification method and the corresponding computational formula based on the static testing method. However, the effects of flexural rigidity cannot be ignored in practical cable force identification because the cable segment fixed by the clamp is usually short (Ceballos and Prato 2008, Park and Kim 2014).

The calculation results of Eq. (1) and Eq. (2) are corrected by calibration test to solve the above problem. To overcome the limitations, the effect of flexural rigidity in cable force identification is taken into consideration in this paper.

To investigate the effects of flexural rigidity, a mechanical analysis model of the fixed cable segment is founded. As shown in Fig. 2, both ends of the cable are rigid embedded. T_0 is the tension force of the cable segment. N is the jacking force at mid-span, and T is the horizontal force of support. The deformed cable is put in a rectangular plane coordinate system, and x is the distance from the calculated section to the left end. z is the vertical displacement of the cable, and l is the original length of the cable segment.

According to the principle of static equilibrium, it can be obtained as follows

$$0 \le x \le \frac{l}{2}, M_x = \frac{Nx}{2} - M_0 - Tz \quad (3)$$

Based on small deflection differential equation of elastic curve, it can be got as follows

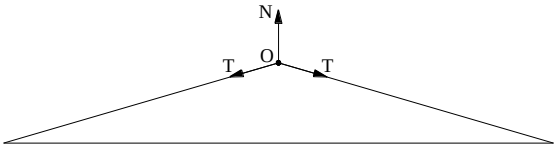

Fig. 3 Deformation of the ideal flexible cable

$$\frac{d^2z}{dx^2} = -\frac{M_x}{EI} \tag{4}$$

$$\frac{d^2z}{dx^2} - \frac{Tz}{EI} = -\frac{Nx}{2EI} + \frac{M_x}{EI} \tag{5}$$

Assume $r^2 = \frac{T}{EI}(r > 0)$, then the general solution of Eq. (5) is

$$z = c_1 e^{-rx} + c_2 e^{rx} \tag{6}$$

The particular solution of Eq. (5) is assumed to be $z^* = a_1 x + a_2$. Then z^* is taken into Eq. (5)

$$-\frac{T}{EI}(a_1 x + a_2) = -\frac{Nx}{2EI} + \frac{M_0}{EI} \tag{7}$$

The solution of Eq. (7) is

$$a_1 = \frac{N}{2T}, a_2 = -\frac{M_0}{T} \tag{8}$$

Then,

$$z = c_1 e^{-rx} + c_2 e^{rx} + \frac{Nx}{2T} - \frac{M_0}{T} \tag{9}$$

According to the left boundary conditions, that is $x = 0, z = 0$. Then substitute into Eq. (9)

$$0 = c_1 + c_2 - \frac{M_0}{T} \tag{10}$$

In addition, the derivation of Eq. (9) is

$$z' = -rc_1 e^{-rx} + rc_2 e^{rx} + \frac{N}{2T} \tag{11}$$

According to left boundary conditions, the following can be inferred

$$0 = -\mathrm{r}c_1 + rc_2 + \frac{N}{2T} \tag{12}$$

Combining Eq. (10) and Eq. (12), it can be obtained as follows

$$c_1 = \frac{M_0}{2T} + \frac{N}{4Tr} \tag{13}$$

$$c_2 = \frac{M_0}{2T} - \frac{N}{4Tr} \tag{14}$$

Then z and z' can be obtained by substituting c_1 and c_2 into Eq. (9) and Eq. (11)

$$z = \left(\frac{M_0}{2T} + \frac{N}{4Tr}\right)e^{-rx} + \left(\frac{M_0}{2T} - \frac{N}{4Tr}\right)e^{rx} + \frac{N}{2T}x - \frac{M_0}{T} \tag{15}$$

$$\mathrm{z}' = -\mathrm{r}\left(\frac{M_0}{2T} + \frac{N}{4Tr}\right)e^{-rx} + r\left(\frac{M_0}{2T} - \frac{N}{4Tr}\right)e^{rx} + \frac{N}{2T} \tag{16}$$

According to the middle boundary conditions, $x = \frac{l}{2}, z' = 0$, that is,

$$0 = -\mathrm{r}\left(\frac{M_0}{2T} + \frac{N}{4Tr}\right)e^{-r\frac{l}{2}} + r\left(\frac{M_0}{2T} - \frac{N}{4Tr}\right)e^{r\frac{l}{2}} + \frac{N}{2T} \tag{17}$$

and its solution is

$$M_0 = \frac{N(e^{r\frac{l}{2}} + e^{-r\frac{l}{2}} - 2)}{2r(e^{r\frac{l}{2}} - e^{-r\frac{l}{2}})} \tag{18}$$

The following result can be obtained by substituting Eq. (18) into Eq. (15)

$$z = \frac{N}{2Tr}\left(\frac{e^{r\frac{l}{2}} - 1}{e^{r\frac{l}{2}} - e^{-r\frac{l}{2}}}\right)e^{-rx} + \frac{N}{2Tr}\left(\frac{e^{-r\frac{l}{2}} - 1}{e^{r\frac{l}{2}} - e^{-r\frac{l}{2}}}\right)e^{rx} + \frac{N}{2T}x - \frac{N}{2Tr}\left(\frac{e^{r\frac{l}{2}} + e^{-r\frac{l}{2}} - 2}{e^{r\frac{l}{2}} - e^{-r\frac{l}{2}}}\right) \tag{19}$$

Let $z_1 = \frac{N}{2T}x$, then

$$z_2 = \frac{N}{2Tr}\left(\frac{e^{r\frac{l}{2}} - 1}{e^{r\frac{l}{2}} - e^{-r\frac{l}{2}}}\right)e^{-rx} + \frac{N}{2Tr}\left(\frac{e^{-r\frac{l}{2}} - 1}{e^{r\frac{l}{2}} - e^{-r\frac{l}{2}}}\right)e^{rx} - \frac{N}{2Tr}\left(\frac{e^{r\frac{l}{2}} + e^{-r\frac{l}{2}} - 2}{e^{r\frac{l}{2}} - e^{-r\frac{l}{2}}}\right) \tag{20}$$

Thus, Eq. (19) becomes

$$z = z_1 + z_2 \tag{21}$$

Fig. 3 shows the deformation of the ideal flexible cable with force at the mid-span, and the cables on both sides remain straight. At the force point O, the following can be obtained

$$2T\sin\theta = N \Longrightarrow \sin\theta = \frac{N}{2T} \tag{22}$$

As θ is small enough, it can be obtained that $\sin\theta \approx \tan\theta \approx \theta$. The deformation curve without considering flexural rigidity can be expressed as

$$z = x\tan\theta = \frac{N}{2T}x \tag{23}$$

z is the same as z_1. Thus, z_1 reflects the characteristics of the flexible cable, while z_2 represents the effect of flexural rigidity on the lateral jacking deformation of cable segment.

According to Eq. (19), when $x = \frac{l}{2}$, the followings can be obtained

$$z_1 = \frac{Nl}{4T} \tag{24}$$

$$z_2 = \frac{N}{Tr}\left(\frac{2 - e^{-r\frac{l}{2}} - e^{r\frac{l}{2}}}{e^{r\frac{l}{2}} - e^{-r\frac{l}{2}}}\right) \tag{25}$$

The flexural stiffness correction coefficient is defined as

$$\alpha = \frac{z_2}{z_1} = \frac{4}{lr}\left(\frac{2 - e^{-r\frac{l}{2}} - e^{r\frac{l}{2}}}{e^{r\frac{l}{2}} - e^{-r\frac{l}{2}}}\right) \tag{26}$$

Thus, the mid-span displacement of the cable segment can be expressed as

$$z = \frac{Nl}{4T}(1 + \alpha) \tag{27}$$

The following result can be obtained by substituting the boundary condition $x = \frac{l}{2}, z = \delta$ into Eq. (19)

$$e^{r\frac{l}{2}} = \frac{1 - \frac{\delta Tr}{N} + \frac{lr}{4}}{1 + \frac{\delta Tr}{N} - \frac{lr}{4}} \tag{28}$$

Function $T(N, \delta)$ can be obtained by solving Eq. (28), and $z(N, \delta, x)$can be obtained by substituting $T(N, \delta)$ into Eq. (19). As the lateral jacking displacement is extremely small, the axial tension is supposed to be equal to the horizontal force of supports T. Through measuring the elongation of the fixed cable segment, the implicit formula of the cable force can be obtained as follows

$$\frac{T(N, \delta) - T_0}{EA} \times \frac{l}{2} = \int_0^{\frac{l}{2}} \sqrt{1 + (z'(N, \delta, x))^2}\, dx - \frac{l}{2} \tag{29}$$

4. Solution of cable force identification formula considering flexural rigidity

Considering the difficulty in separating $T(N, \delta)$ from Eq. (28) and calculating the integral of Eq. (29), the numerical method is applied to solve the initial cable force (T).

Through numerical method, the followings can be obtained by substituting $r = \sqrt{\frac{T}{EI}}$ into Eq. (28)

$$\begin{aligned} &e^{\frac{l}{2}\sqrt{\frac{T}{EI}}}\left(1 + \frac{\delta}{N}\sqrt{\frac{T^3}{EI}} - \frac{l}{4}\sqrt{\frac{T}{EI}}\right) \\ &\quad - \left(1 - \frac{\delta}{N}\sqrt{\frac{T^3}{EI}} + \frac{l}{4}\sqrt{\frac{T}{EI}}\right) = 0 \end{aligned} \tag{30}$$

Let $f(T) = e^{\frac{l}{2}\sqrt{\frac{T}{EI}}}\left(1 + \frac{\delta}{N}\sqrt{\frac{T^3}{EI}} - \frac{l}{4}\sqrt{\frac{T}{EI}}\right) - \left(1 - \frac{\delta}{N}\sqrt{\frac{T^3}{EI}} + \frac{l}{4}\sqrt{\frac{T}{EI}}\right)$, then the first derivation of $f(T)$ is

$$\begin{aligned} f'(T) = {} & e^{\frac{l}{2}\sqrt{\frac{T}{EI}}}\left(\frac{1}{4\sqrt{EIT}} + \frac{\delta lT}{4NEI} - \frac{l^2}{16EI}\right) + \\ & e^{\frac{l}{2}\sqrt{\frac{T}{EI}}}\left(\frac{3\delta}{2N}\sqrt{\frac{T}{EI}} - \frac{1}{8\sqrt{EIT}}\right) + \frac{3\delta}{2N}\sqrt{\frac{T}{EI}} - \frac{1}{8\sqrt{EIT}} \end{aligned} \tag{31}$$

Use Newton iterative method with

$$T_{k+1} = T_k - \frac{f(T_k)}{f'(T_k)}\ (k = 0,1,2\cdots) \tag{32}$$

As the cable force is usually less than 20%-40% of its ultimate bearing capacity in practice according to design specification (Chen *et al.* 2015, Kaveh and Rezaei 2015), the iterative initial values T_0 is assumed to be $0.3 f_{ptk} A$.

Iteration will stop when $\frac{\|T_{k+1} - T\|_k}{T_{k+1}} \le \varepsilon$, and $T = T_{k+1}$. When T is taken into Eq. (19), the displacement curve $z(x)$ of the cable after being jacked can be obtained. When T is taken into Eq. (16) and Eq. (18), the slope $z'(x)$ of the curve can be obtained.

In Eq. (29), N and δ can be measured with devices. The cable is divided into 2n parts to calculate $\int_0^{\frac{l}{2}} \sqrt{1 + (z'(x))^2}\, dx$ and T_0.

$$\begin{aligned} &\int_0^{\frac{l}{2}} \sqrt{1 + (z'(x))^2}\, dx \\ &\approx \left(\sqrt{1 + \left(z'(0)\right)^2}\right. \\ &\quad \left. + \sqrt{1 + (z'(\frac{l}{2}))^2}\right) \\ &\times \frac{l}{4n} + \sum_{k=1}^{n-1} \sqrt{1 + (z'(\frac{lk}{2n}))^2}\, \frac{l}{2n} \end{aligned} \tag{33}$$

$$\begin{aligned} T_0 \approx {} & T - \frac{2EA}{l}\left(\sqrt{1 + \left(z'(0)\right)^2}\, \frac{l}{4n}\right. \\ & \left. + \sqrt{1 + (z'(\frac{l}{2}))^2}\, \frac{l}{4n}\right. \\ & \left. + \sum_{k=1}^{n-1} \sqrt{1 + (z'(\frac{lk}{2n}))^2}\, \frac{l}{2n} - \frac{l}{2}\right) \end{aligned} \tag{34}$$

For convenient calculation, a dedicated calculation program called Pretension Identification of Cable based on Static Equilibrium Method (PTICBSM) is established on the basis of Fortran.

5. Verification of calculation example

A series of numerical experiments of general finite element analysis software ABAQUS and PTICBSM are used to assess the feasibility of the cable force identification method considering flexural rigidity. In numerical experiment, a 1000-mm long cable with 20-mm diameter is

Table 1 Comparisons between numerical experimental results of ABAQUS and calculation results of PTICBSM

Jacking displacement (mm)	Jacking force (kN)	Cable force of cable segment when jacked (kN)		Initial cable force (kN)		Identification error of cable force
		Numerical experiment	PTICBSM	Numerical experiment	PTICBSM	
2	1.48	122.4	120.7	122.1	120.3	1.47%
4	2.99	123.5	122.3	122.1	120.9	0.98%
6	4.53	125.2	124.0	122.1	120.7	1.14%
8	6.13	127.7	126.4	122.1	120.7	1.14%
10	7.80	130.8	129.4	122.1	120.6	1.22%
12	9.57	134.6	133.3	122.1	120.5	1.31%
14	11.45	139.2	137.8	122.1	120.4	1.39%
16	13.46	144.4	142.9	122.1	120.3	1.47%
18	15.62	150.2	148.9	122.1	120.2	1.55%
20	17.94	156.8	155.3	122.1	120.0	1.72%

Table 2 Parameters of cables

A (mm^2)	E (N/mm^2)	EI (N×mm^2)	f_{ptk} (MPa)	$0.3f_{ptk}A$ (kN)	L (mm)
244.16	1.6×10^5	9.24×10^8	1670	122	1000

Table 3 L/A of tested cable segment with different lengths

L (mm)	1000	1500	2000	2500	3000	3500	4000	4500	5000
L/A(mm^{-1})	4.10	6.14	8.19	10.24	12.29	14.33	16.38	18.43	20.48

chosen as the test model. The prestressed force is $0.3f_{ptk}A$. Considering the tension state and sectional geometrical feature of prestressed cable, beam element which can bear both bending moment and axial tension is reasonable to be applied to simulate the cable under the tension state (unrelaxed state) during the modeling in ABAQUS. According to the cable sectional area and principle of one-way equivalent flexural rigidity, element B21 in ABAQUS is chosen and the initial tension is applied in the form of an equivalent temperature load. Table 1 presents comparisons between numerical experimental results of ABAQUS and calculation results of PTICBSM. Table 2 shows parameters of the cables.

The analysis shows that the results from PTICBSM are in agreement with the numerical experimental results. The proposed method has high computational accuracy and can be used to identify the cable force in practice.

To evaluate the effects of flexural rigidity, the cables with 20mm diameter are used and the cable segments with different lengths are also investigated. As shown in Table 3, the initial tension is $0.15f_{ptk}A$, $0.30f_{ptk}A$, and $0.45f_{ptk}A$, respectively, that is, 61 kN, 122 kN and 183 kN, and the jacking rise span ratio is 1%.

Fig. 4 shows the error between the results of finite element method and the results of the cable force identification method without considering flexural rigidity. It is indicated that if the L/A (ratio of cable length to sectional area) is larger, the error is smaller. When L/A remains unchanged, if tension T_0 is smaller, the error becomes larger. In this calculation example, if $T_0 \geq 0.30f_{ptk}A$, L/A must exceed 16 (mm^{-1}) to ensure that the error is less

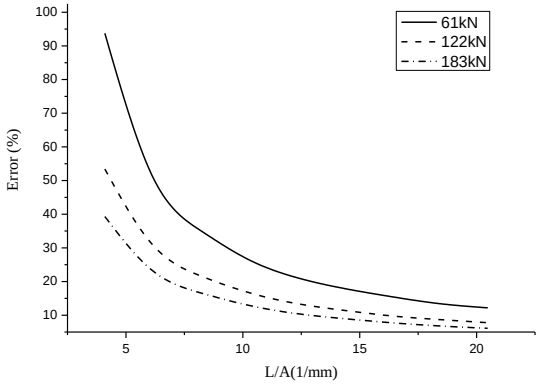

Fig. 4 Error analysis of the cable force identification without considering flexural rigidity

than 10%, and the length of the test cable should be not less than 3.9 m. Similarly, if the diameters of the cables are 36 mm and 48 mm, when $T_0 \geq 0.30f_{ptk}A$, L/A must exceed 9.4 (mm^{-1}) and 7.1 (mm^{-1}) to ensure that the error is less than 10%, and the length of the test cable should be not less than 7.2 m and 9.8 m. For convenient operation or limited field condition in practice, the actual length of the fixed cable segment is extremely small, which leads to a large error through the cable force identification method without considering flexural rigidity. Thus, the effects of flexural rigidity cannot be ignored in practical cable force identification.

6. Experiment on cable force identification

6.1 Experimental introduction

In order to investigate the influence of flexural rigidity of the cable in actual cable testing process, the experiment of a short fixed cable segment is carried out. Three kinds of cables with diameters of φ20, φ36 and φ48 are used and mixed rare earth alloy coating cables are applied in the experiment. The length of the fixed cable segment is 1000 mm. When the cable force increases, the cable segment can be fixed by the cable clamp to avoid relative slip between

Table 4 Design parameters of the cable clamp

Cable clamp size (mm) \ Cable diameter	φ20	φ36	φ48
Width a	70	90	100
Height b	20	30	38
Gap d	6	6	6
Length l	80	80	80
Inner diameter of brass pad r	10	18	24
Thickness of brass pad t	2	2	2

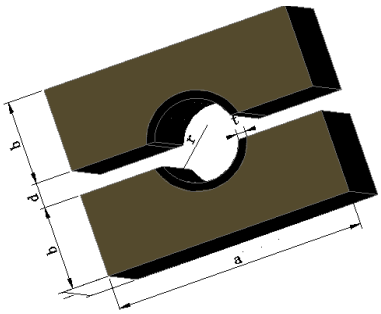

Fig. 5 Configuration of the composite cable clamp

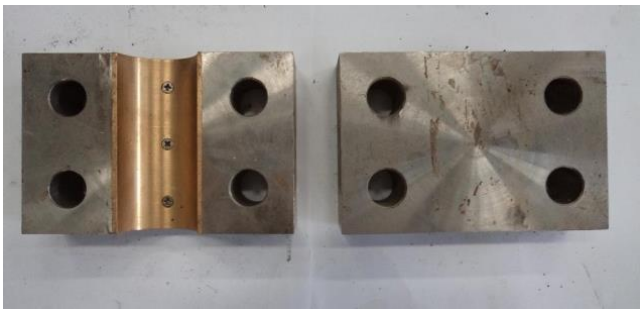

Fig. 6 Composite cable clamp

the cable and the cable clamp. The cable force increment of cable segment will not be transferred to the lateral cable segments. A special composite cable clamp (40 Cr tempered steel + brass) is used. Table 4 and Fig. 5 show the design parameters and configuration of the composite cable clamp. Fig. 6 is the actual picture of the composite cable clamp.

As shown in Table 5, three groups of samples are included in the experiment, and each group has six levels of initial cable force.

6.2 Experimental method and steps

Fig. 7 shows the experimental device. Two sets of cable clamp are installed in different sides of the jacking point, and the distance between the two clamps is 1000 mm. The cable clamp is used to fix the cable in certain position. The cable clamp is fixed in the self-balancing loading device to avoid horizontal and vertical displacement of the cable clamp. Initial cable force T_0, jacking force F, and jacking displacement δ are needed to be recorded.

As shown in Fig. 8, jacking force is measured by a pressure sensor, and jacking displacement of force point is measured by a dial indicator, the followings are the specific experimental steps:

Table 5 Load cases of cable force identification experiment

Diameter	T_0(kN)					
	LC1	LC2	LC3	LC4	LC5	LC6
φ20	104.52	106.15	127.74	130.60	149.53	153.59
φ36	311.28	315.58	379.85	387.50	438.00	449.68
φ48	445.45	447.58	524.67	530.90	557.54	567.30

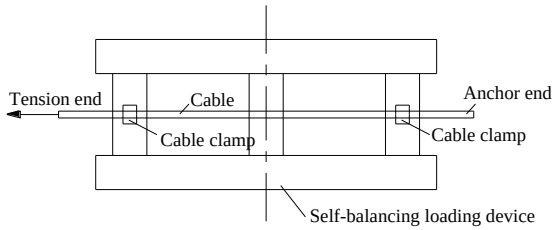

(a) Plan view of experimental device

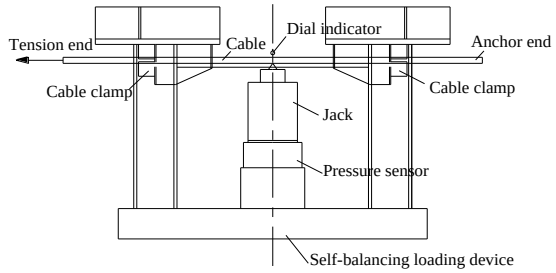

(b) Vertical view of experimental device

Fig. 7 Diagram of cable force identification experiment

Fig. 8 Experiment of cable force identification

(1) The cable is installed and the initial cable force T_0 is applied.

(2) The cable clamp is installed corresponding to the diameter of the cable and the cable clamp is fixed in the self-balancing loading device.

(3) The pressure sensor and jack are installed, and the jack is lifted slowly until the jacking device touches the cable.

(4) The dial indicator is installed and its initial reading is obtained.

(5) The jack is lifted step by step and the readings of the dial indicator and pressure sensor are recorded.

(6) The initial cable force is applied according to the

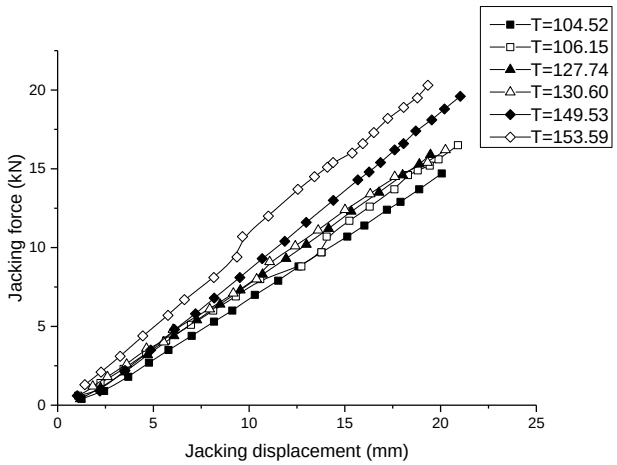

Fig. 9 Relation curve between jacking displacement and jacking force of φ20

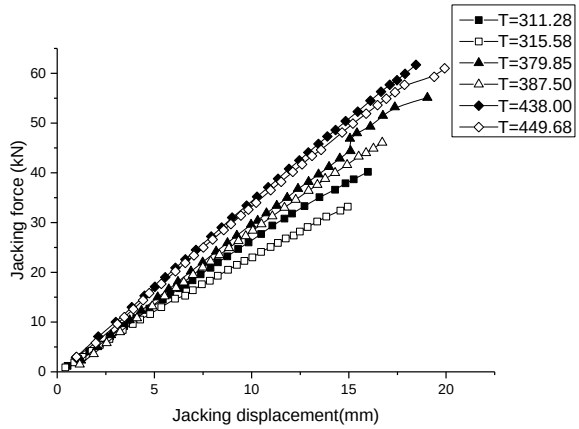

Fig. 10 Relation curve between jacking displacement and jacking force of φ36

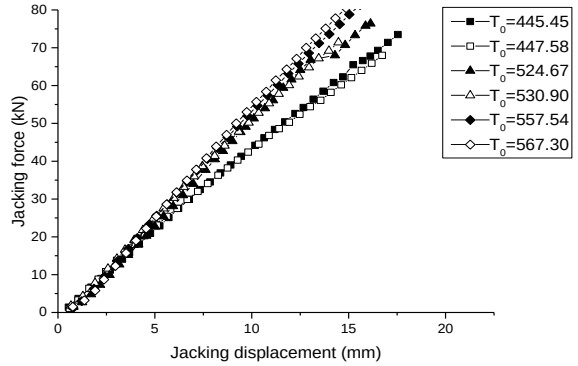

Fig. 11 Relation curve between jacking displacement and jacking force of φ48

load cases which are shown in Table 5. The above steps are repeated and the data are collected.

6.3 Experimental result and analysis

6.3.1 Relation between jacking displacement and jacking force

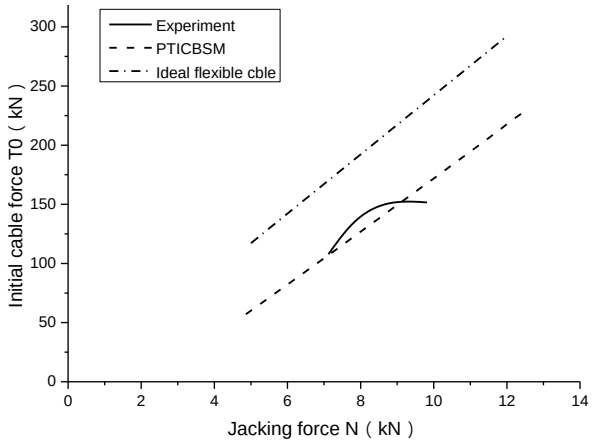

Fig. 12 Relation between initial cable force and jacking force when jacking displacement δ is equal to 10 mm

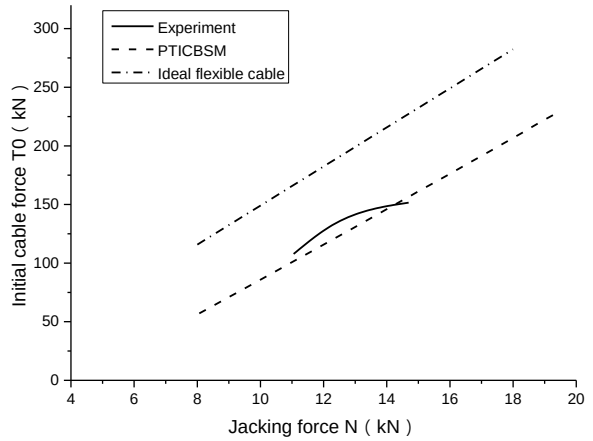

Fig. 13 Relation between initial cable force and jacking force when jacking displacement δ is equal to 15 mm

Figs. 9-11 show the relation curve between jacking displacement and jacking force on the force point of cables φ20, φ36, and φ48 when the initial cable force differs.

The results can be obtained as follows:

1) When the initial tension (T_0) is a constant, the jacking displacement and jacking force obey the linear relationship, that is, increased jacking displacement corresponds to increased jacking force.

2) When the cable cross section (A) is a constant, the cable with larger sectional area corresponds to larger jacking force, which owes to the increased effect of flexural rigidity.

3) If the cable is assumed to be ideal flexible, for different cable cross section (A), when the initial cable force (T_0) remains constant and the jacking displacement (δ) is the same, the relationship between the cable cross section and jacking force can be obtained as follows

$$\frac{\Delta N}{\Delta A} = 8E(\frac{\delta}{L})^3 = constant \tag{36}$$

It means that the jacking force increases linearly with the increase of the cable cross section. When the same jacking displacement is needed, the jacking force of the

cable with larger cross section increases faster. It reflects that the effects of flexural rigidity increases with the increase of the cable cross section.

6.3.2 Relation between initial cable force and jacking force

Figs. 12 and 13 present comparison among the experimental data, the calculation results from PTICBSM and the cable force identification formula (without considering flexural rigidity) proposed by Wang *et al.* (2013) with cable φ20.

The results show the following:

(1) When the jacking displacement δ and jacking force F is constant, the tension from formula made by Wang *et al.* (2013) is larger than the calculation value of PTICBSM. The reason is that the fixed cable segment is extremely short, and the cable flexural rigidity has great influence on the calculation of cable force T_0.

(2) Compared with the experimental results, the error of the results made by Wang *et al.* (2013) is larger and the average errors are 51.87% and 48.73%, respectively. The results of PTICBSM are in good agreement with the experimental results, and the average errors are only 6.56% and 6.16%, respectively. The results prove that the calculation method considering flexural rigidity is much more consistent with the actual state of the cable, and it can be applied in practice.

(3) With the proposed method in this paper, it is necessary to guarantee that no relative sliding occurs between the cable and the cable clamp. When the jacking rise span ratio is small (1% to 1.5%), the clamps are able to provide sufficient friction and the experimental value is close to the calculation value of PTICBSM. However, when the jacking rise span ratio increases, the error would increase due to insufficient friction. Therefore, in the process of cable force identification, the friction between the cable and the cable clamp must be sufficient by controlling the quality of cable clamp, and jacking rise span ratio should be ranged from 1% to 1.5%.

7. Conclusions

• The computational formula for the cable force identification considering flexural rigidity is investigated, and the calculation program PTICBSM based on the computational formula is used to identify the cable force. This study shows that the results of PTICBSM are extremely in good agreement with the finite element results. The proposed method has high computational accuracy and high resolution efficiency. It can be used to identify cable force in practice.

• The relationship and variation law among jacking force, jacking displacement, initial cable force and sectional area (flexural rigidity) are studied with the cable force identification experiments of different cross sections. The results show that when the initial tension remains constant, the jacking displacement and jacking force basically obey linear relation. When the initial tension is constant, the cable with a larger sectional area requires larger jacking force, which owes to the increased effects of flexural rigidity. When the cable section is constant, the cable with larger initial tension requires stronger top jacking force, which owes to the influence of stress stiffening effect.

• Compared with common cable force identification formula under ideal flexible condition, the cable force identification formula considering the effects of flexural rigidity has higher accuracy. Errors are large when the effects of flexural rigidity are not considered, while results from the cable force identification formula considering flexural rigidity are in good agreement with experimental results. It reflects that the method proposed in this paper is consistent with the actual condition of the cable. The cable force identification method considering flexural rigidity is proven to be accurate and feasible. In addition, the experimental results show that during actual cable force testing, the friction between the cable and the cable clamp must be sufficient by controlling the quality of the cable clamp, and the jacking rise span ratio should be ranged from 1% to 1.5%.

Acknowledgments

The research described in this paper was financially supported by the Opening Project of State Key Laboratory of Subtropical Building Science, South China University of Technology, China (Grant No. 2012KB31) and the Science and Technology Program of Guangzhou, China (Grant No. 1563000257).

References

Amabili M., Carra S., Collini L., Garziera R. and Panno A. (2010), "Estimation of tensile force in tie-rods using a frequency-based identification method", *J. Sound Vibr.*, **329**(11), 2057-2067.

Ceballos M.A. and Prato C.A. (2008), "Determination of the axial force on stay cables accounting for their bending stiffness and rotational end restraints by free vibration tests", *J. Sound Vibr.*, **317**(1), 127-141.

Chen L.M, Zhou Y.Y. and Dong S.L. (2015), "Overall self-stress modes analysis and optimal prestress design of the Kiewitt dome", *J. Int. Assoc. Shell Spat. Struct.*, **56**(2), 113-123.

Kaveh A. and Rezaei M. (2015), "Optimum topology design of geometrically nonlinear suspended domes using ECBO", *Struct. Eng. Mech.*, **56**(4), 667-694.

Kim S. and Kang Y.J. (2016), "Structural behavior of cable-stayed bridges after cable failure", *Struct. Eng. Mech.*, **59**(6), 1095-1120.

Park D.U. and Kim N.S. (2014), "Back analysis technique for tensile force on hanger cables of a suspension bridge", *J. Vibr. Contr.*, **20**(5), 761-772.

Rebelo, C., Julio, E., Varum, H. and Costa, A. (2010), "Cable tensioning control and modal identification of a circular cable-stayed footbridge", *Exp. Technol.*, **34**(4), 62-68.

Russell, J.C. and Lardner, T.J. (1998), "Experimental determination of frequencies and tension for elastic cables", *J. Eng. Mach.*, **124**(10), 1067-1072.

Shu, Y.J., Chen, W.M. and Wu, J. (2013), "Embedding technology of Fiber Bragg Grating strain sensor for cable tension monitor", *Proceedings of the SPIE-The International Society for Optical Engineering*, Beijing, China, December.

Sim, S.H., Li, J., Jo, H., Park, J.W., Cho, S., Spencer Jr, B. and Jung, H.J. (2014), "A wireless smart sensor network for

automated monitoring of cable tension", *Smart Mater. Struct.*, **23**(2), 025006.
Tang, D., Zhu, H., Mou, J. and Wu, M. (2014), "Research on the temperature influence and compensation technique in a magneto-elastic cable tension sensor", *Int. J. Sens. Netw.*, **16**(4), 236-243.
Tian G.Y., Guo Y.L., Zhang B.H. and Wang K. (2013), "Research on error of a cable force estimation method for spoke structural roofs", *Eng. Mech.*, **30**(3), 126-132.
Wang, J., Liu, W.Q., Wang, L. and Han, X. (2015), "Estimation of main cable tension force of suspension bridges based on ambient vibration frequency measurements", *Struct. Eng. Mech.*, **56**(6), 939-957.
Wang, L., Wu, B., Gao, J.Y. and Wang, F. (2013), "Tension identification of in-service cable by static equilibrium method", *J. Chongqing Univ.*, **36**(8), 125–132.
Xia, Q., Wu, J.J., Zhu, X.W. and Zhang, J. (2017), "Experimental study of vibration characteristics of FRP cables based on Long-Gauge strain", *Struct. Eng. Mech.*, **63**(6), 735-742.
Zhang, Y.X., Li, G.Q., Liu, H.C. (2006), "Cable force identification of beam string structures based on static measuring methods", *Spec. Struct.*, **23**(4), 54-55.
Zhu, Z.Y., Sun, G.M., Wu, B., He, C., Li, Y., Liu, X. and Wu, D. (2018), "A temperature compensation method for magneto-elastic tension sensor in rod-like structure tension measurement", *IEEE Trans. Mag.*, **54**(4), 1-16.

CC